DTD 5
ARTICLE IN PRESS

Available online at www.sciencedirect.com
SCIENCE DIRECT®

Dynamics of Atmospheres and Oceans
xxx (2005) xxx–xxx

dynamics of atmospheres and oceans

www.elsevier.com/locate/dynatmoce

Dynamical elements of predicting boreal spring tropical Atlantic sea-surface temperatures

M. Barreiro[a,*], P. Chang[a], L. Ji[a], R. Saravanan[b], A. Giannini[c]

[a] *Department of Oceanography, Texas A&M University, College Station, TX 77843-3146, USA*
[b] *National Center for Atmospheric Research, Boulder, CO 80307-3000, USA*
[c] *International Research Institute for Climate Prediction, Columbia University, Palisades, NY, 10964-8000, USA*

Received 5 December 2003; accepted 5 October 2004

Abstract

The dynamical processes that contribute to the seasonal prediction of the tropical Atlantic sea-surface temperature (SST) anomalies from boreal winter into spring are explored with an atmospheric general circulation model coupled to a slab ocean. Taking advantage of the reduced-physics model that effectively isolates thermodynamic feedbacks from dynamic feedbacks, we examine the joint effect of local thermodynamic feedback and the remote influence of El Niño-Southern Oscillation (ENSO) on the prediction of SST anomalies by conducting large ensembles of prediction runs. These prediction experiments yield the following findings: (1) in the northwestern part of the tropical Atlantic, the positive feedback between the surface heat flux and SST can play an important role in enhancing the predictability of the SST; (2) the remote influence from Pacific ENSO can enhance the SST predictability through a constructive interference with the local thermodynamic feedback, but can also make the SST prediction more difficult when the interference is destructive; (3) ocean dynamics plays a fundamental role for prediction of SST anomalies in the equatorial and south tropical Atlantic. To shed further light on the importance of the ocean dynamics, a statistical procedure of parameterizing the important ocean dynamics is developed within a linear dynamical framework. Prediction experiments with the parameterized ocean dynamics included in the simple coupled model result in an improved forecast skill in predicting the cross-equatorial SST gradient, which subsequently lead to a high skill of the model in predicting seasonal rainfall anomalies associated with variations in the Intertropical Convergence Zone during boreal spring. A diagnostic study suggests that the vertical advection of heat

* Corresponding author. Now at Program in Atmospheric and Oceanic sciences, Princeton University, Princeton, NJ 08544-0710, USA. Tel.: +1 609 258 1319; fax: +1 609 258 2850.
E-mail address: barreiro@princeton.edu (M. Barreiro).

0377-0265/$ – see front matter
doi:10.1016/j.dynatmoce.2004.10.013

due to anomalous Ekman pumping/suction is a dominant contributing factor for causing equatorial SST anomalies, thereby, a major element of predictable dynamics in this region.

Keywords: Sea-surface temperature; Tropical Atlantic; Prediction; Thermodynamic feedback; ENSO

1. Introduction

The current success of seasonal climate prediction is largely limited to the El Niño-Southern Oscillation (ENSO) phenomenon in the tropical Pacific. Extending seasonal climate forecasts beyond ENSO remains a great challenge for climate researchers, because climate variability outside of the tropical Pacific depends not only on ENSO, but also on other regional phenomena that interact with ENSO. Perhaps the most notable of these is the Tropical Atlantic Variability (TAV), which is known to have a significant impact on precipitation over the Northern Nordeste region of Brazil and the Sahel region of Africa (Hastenrath and Heller, 1977; Folland et al., 1986). Both the Sahel and the Northern Nordeste are semi-arid, drought-prone regions. Therefore, predicting rainfall variation at seasonal timescales in these regions has important human consequences.

It has become increasingly evident that predicting El Niño-related sea-surface temperature (SST) variability in the tropical Pacific alone is not sufficient to make an accurate seasonal climate forecast over the tropical Atlantic sector, even though ENSO does contribute significantly to climate variability in that region. As an example to illustrate this point, Fig. 1 shows a comparison between observed and simulated indices of Nordeste rainfall during boreal spring, March–April–May (MAM), over the past five decades. The

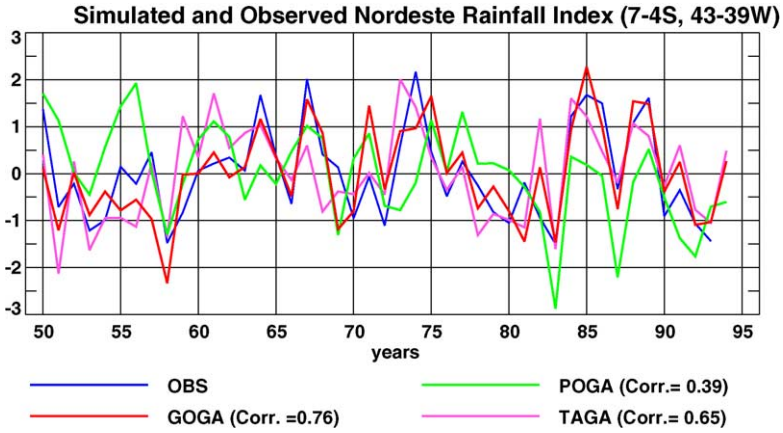

Fig. 1. Simulated and observed NE Brazil rainfall index. Simulations are based on the CCM3 forced by observed SST in various ocean basins. Blue, observation; red, global SST; green, tropical Pacific-only SST; magenta, tropical Atlantic-only SST. Correlations among different simulations and observations are listed at the bottom of each panel.

atmospheric general circulation model used here was the Community Climate Model version 3.6.6 (CCM3) developed at the National Center for Atmospheric Research. When global SST is used to force the CCM3 (Global Ocean–Global Atmosphere or GOGA runs), the simulated rainfall index (red) tracks closely the observed index (blue) and correlation between the two achieves a high value of 0.76. In contrast, when only tropical Pacific SST is used to force CCM3 while SSTs in other ocean basins are set to climatological values (Pacific Ocean–Global Atmosphere or POGA runs), the correlation between the observed and simulated (green) indices drops below 0.4. Interestingly, when only tropical Atlantic SST is used to force CCM3 (Tropical Atlantic–Global Atmosphere or TAGA runs), the correlation between the observed and simulated (magenta) retains a value of 0.65. This suggests that SST anomalies in the tropical Atlantic Ocean are crucial for seasonal climate forecasting in the region. That said, it is worth emphasizing that SST conditions in the tropical Atlantic depend on both local feedbacks and remote influence from other phenomena, such as ENSO. Therefore, ENSO can affect TAV not only directly through an atmospheric bridge (Klein et al., 1999) but also indirectly through interaction with local feedbacks which modify tropical Atlantic SST.

Our current ability to forecast the tropical Atlantic SST anomaly is very limited (Penland and Matrosova, 1998; Goddard et al., 2001). This is partly due to the fact that the dynamics governing SST variability is complex and still poorly understood. Although, it is now widely recognized that SST variability in the tropical Atlantic is affected by both local air–sea feedbacks and remote influences from ENSO and extratropical atmospheric variability, much still needs to be learned about their details and about interactions between them. The other major obstacle for a skillful forecast in the tropical Atlantic Ocean is that the current generation of coupled climate models shows significant systematic biases in the region (Davey et al., 2002).

The complexity of SST dynamics is manifested by the multiple patterns of SST variability that can be distinguished by season, location, underlying physics and the subsequent impact on society. Among them, two have received most attention:

- A pattern of a north–south SST gradient coupled with a cross-equatorial circulation in the lower atmosphere which peaks in the boreal spring and continues into the early summer. This so-called “meridional mode” involves a local interaction between SST, wind, and convection in the western equatorial Atlantic and affects primarily regional climate in the vicinity of Brazil. The local air–sea interaction is shown to produce a positive feedback during the boreal spring, affecting the length of the rainy season in the semi-arid region of northeast Brazil (Chang et al., 2000; Chiang et al., 2002). What is well known about this mode is that Pacific ENSO and the North Atlantic Oscillation can both have a remote influence on its time evolution (Enfield and Mayer, 1997; Saravanan and Chang, 2000; Czaja et al., 2002). These remote influences can interfere with local feedbacks, affecting regional SST conditions, which in turn affect rainfall variability over northeast Brazil (Giannini et al., 2004). What is less known about this mode is the role of ocean dynamics in regulating SST. A number of recent modeling studies (Chang et al., 2001; Seager et al., 2001) suggest that meridional ocean heat transport associated with the mean circulation in the tropical Atlantic tends to counteract the positive feedback, weakening the anomalous cross-equatorial SST gradient forming in the boreal spring.

But the importance of upper-ocean processes in predicting the SST anomaly associated with this mode is unknown.

- A pattern of an equatorial SST anomaly coupled with an equatorial trade wind anomaly, which peaks in the boreal summer and into the fall. This so-called "equatorial mode" (Zebiak, 1993; Carton and Huang, 1994; Ruiz-Barradas et al., 2000) bears a certain resemblance to ENSO where the Bjerknes mechanism is known to be crucially important. It has been noted that precipitation conditions along the upper coast of the Gulf of Guinea during early summer are closely linked to the anomalous SST in the eastern equatorial Atlantic. However, the detailed dynamics of the equatorial mode is still poorly understood, particularly, with respect to the associated subsurface ocean processes and its connection with the remote influence of ENSO. The forecast skill of current climate models for this mode is dismally low for reasons not well understood.

These two phenomena are not necessarily independent of each other. Recent studies suggest that there is a connection between the two patterns in the last 20 years (Servain et al., 2001), but that relationship appears to be absent during the 1950s to 1970s (Murtugudde et al., 2002). The focus of this study is on the meridional mode. We exploit the dynamical processes that contribute to the seasonal prediction of SST anomalies from boreal winter to spring. Our objective is two-fold: (1) to test the hypothesis that both the local feedback and remote influence of ENSO contribute significantly to the predictable dynamics of the SST anomaly associated with the meridional mode and (2) to examine the role of oceanic dynamics in predicting SST anomalies associated with the meridional mode. To achieve these objectives, we conducted sets of prediction experiments with a coupled model of reduced physics that effectively isolates the essential dynamics of the meridional mode from those of the equatorial mode. The arrangement of the paper is as follows. In Section 2, after a short description of the coupled model used in this study, we describe the results of two sets of prediction experiments designed to separate the effect of local feedback and remote influence of ENSO. The results of these experiments will also allow us to identify areas where ocean dynamics are potentially important in seasonal prediction of SST. In Section 3, we attempt to examine the effect of ocean dynamics by introducing a parameterization of ocean dynamics into the coupled model. A comparison of the prediction experiments with the modified coupled model to those with the original model sheds light on the importance of the ocean dynamics. Physical interpretation of the parameterized ocean processes is also discussed. Finally, in Section 4, we summarize major findings and discuss their implications.

2. Role of thermodynamic feedback and remote influence of ENSO

As mentioned above, the thermodynamic feedback and the remote influence of ENSO are two dominant factors affecting the meridional mode. Given that both of these processes are included in an atmospheric general circulation model coupled to a slab ocean, such a simple coupled system can be used to explore the extent to which the meridional mode can contribute to the climate variability and predictability in the tropical Atlantic. One particular advantage of using such a model is that it enables us to isolate the dominant physics associated with the meridional mode from those of the equatorial mode, so that a

deeper understanding of the role of the meridional mode in seasonal prediction of TAV can be gained. Before proceeding to discuss the results of prediction experiments, we give a brief description of the coupled model used in this study.

2.1. Coupled model and prediction experiments

The coupled model used in this study consists of CCM3, version 3.6.6, of the Community Climate Model developed at the National Center for Atmospheric Research (Kiehl et al., 1998), and a simple ocean mixed layer with a spatially varying depth taken from the observed annual mean mixed layer depth (Levitus, 1994). The model (hereafter referred to as CCM3-ML) has a standard resolution—triangular truncation at wavenumber 42 in horizontal and 19 vertical levels. A "q-flux" formulation is used to correct for the absence of ocean dynamics, so that the simulated SST annual cycle is in good agreement with observation. Note that the "q-flux" only takes into consideration the missing oceanic processes for maintaining the annual cycle, but does not represent those oceanic processes that are important to the evolution of SST anomalies.

Two sets of forecast experiments are conducted. In the first set, the mixed layer ocean is initialized with the observed December SST everywhere in the global ocean during the period 1959–2000 (predictions with global initial conditions or PGIC). The coupled CCM3-ML model is then integrated forward for 9 months with 10 sightly different initial conditions for the atmosphere. These initial conditions are derived from the National Center for Environmental Prediction (NCEP) reanalysis (Kalnay et al., 1996) around December 15 of each of the 42 years, thereby representing the actual state of the atmosphere. The second set is identical to the first except the observed SSTs used to initialize the mixed layer ocean are limited to the Atlantic Ocean between 30°S and 60°N (predictions with Atlantic—only initial conditions or PAIC). Outside the Atlantic, the SST anomaly is set to zero everywhere. The purpose of the second set of experiments is to examine the extent to which the predictability can be captured by the thermodynamic feedback between the atmosphere and the mixed layer ocean within the Atlantic basin. A comparison between the two experiments should shed light on the role of ENSO in seasonal prediction of TAV.

The results from these prediction experiments are somewhat astonishing, as shown in Fig. 2. When validating the ensemble mean predictions against the observed SST from the reconstructed data set of Smith et al. (1996), we find that the CCM3-ML has considerable skill in forecasting SST anomaly in the tropical Atlantic during boreal spring. Off-equatorial SST anomalies, particularly those in the tropical north Atlantic (TNA), can be predicted two seasons in advance by CCM3-ML with a high skill. Even in the absence of the direct ENSO influence (PAIC), the model skill is considerably superior to the skill of persistence forecast in the TNA. These results beg for an answer to the following question: what dynamic processes are responsible for the high predictability? We hypothesize that the high predictability is attributable, to a large extent, to the active air–sea feedback between surface heat flux and SST acting in concert with the remote influence of ENSO. In the following subsection, we intend to test this hypothesis by a close examination of the prediction results. Before proceeding, it is worth pointing out another important observation from the twin prediction experiments. That is, in both experiments, the model skill in forecasting equatorial

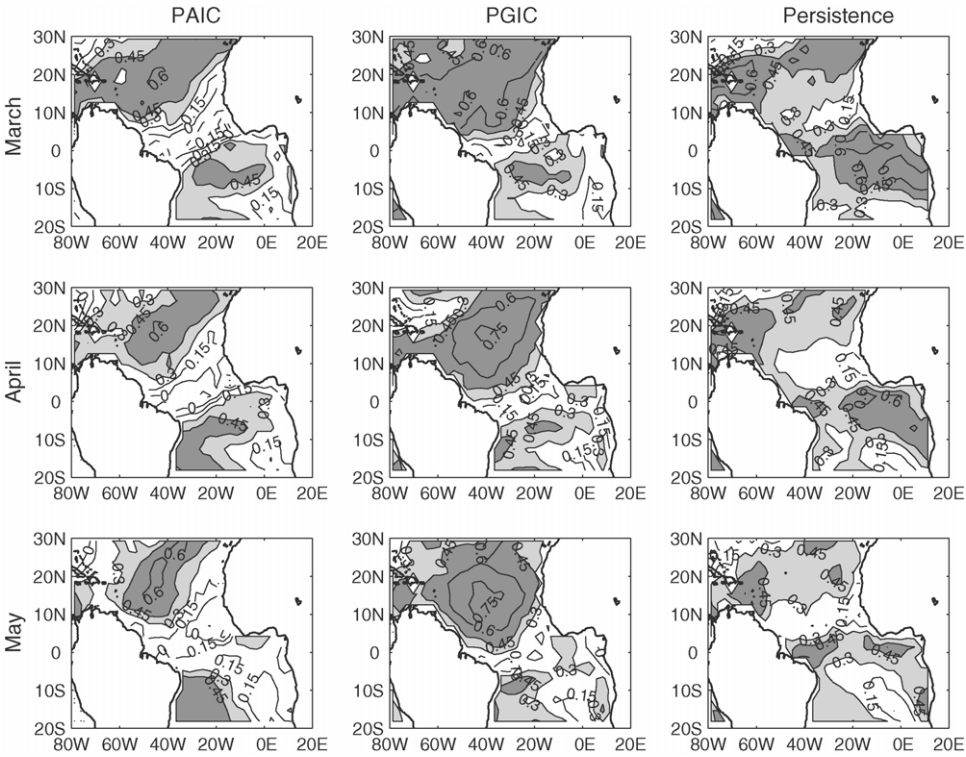

Fig. 2. Correlation skill for PAIC experiment (left panels), PGIC experiment (middle panels) and persistence forecast (right panels) for March, April and May. Correlations larger than 0.3 are in light shading and correlations larger than 0.45 are in dark shading.

and south tropical Atlantic SST is comparatively low (Fig. 2). This points to the potential importance of ocean dynamics in the predictable dynamics of this region, which are entirely absent in the CCM3-ML model. We shall discuss this aspect of the predictable dynamics in Section 3.

2.2. Composite analysis of predictions

To examine the importance of local thermodynamic feedbacks in SST prediction, it is useful to examine the structure of observed SST anomalies in December that are used to initialize the predictions. This is because the effect of the local feedback on SST prediction depends on the initial conditions. If an initial SST anomaly is in favor of the development of the local feedback, then the prediction initialized by this SST anomaly is strongly affected by it. In this particular coupled model, the Wind-Evaporation-SST (WES) feedback which operates primarily on the cross-equatorial SST gradient (Chang et al., 2000) is expected to be the dominant feedback mechanism. Therefore, if the initial SST anomaly has large loading onto a cross-equatorial SST gradient, one expects that the local thermodynamic feedback

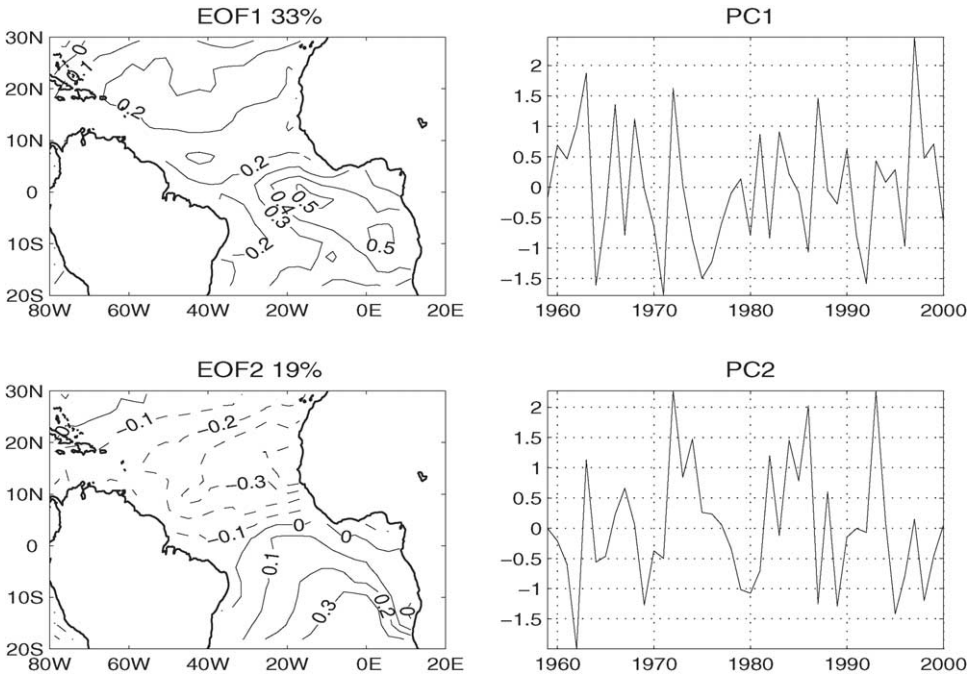

Fig. 3. Leading EOFs of observed December SST. Time series are normalized.

dominates. Furthermore, if these predictions have higher skill than other predictions, then it is reasonable to conclude that the local air–sea feedback is an important contributing factor to the predictable dynamics of SST. On the other hand, if the initial SST condition projects strongly onto a pattern that the coupled model does not support, such as the equatorial mode, then the prediction should have low skills. This reasoning motivates us to perform an empirical orthogonal function (EOF) analysis on the December observed SST anomaly.

Fig. 3 shows the two leading EOFs of the December SST anomaly. The first EOF has a structure with largest weight in the cold tongue region—a feature that characterizes the equatorial mode. The associated principal component (PC) time series gives an indication when this pattern of SST dominates the December SST variability in the tropical Atlantic. The second EOF presents a dipolar pattern with SST maxima off the equator and a large cross-equatorial SST gradient. The associated time series indicates the years when the cross-equatorial SST gradient anomaly is strong during December. The third EOF explains only 10% of the variance with the largest weight north of 20°N, and thus it is not considered here. Using the two leading EOFs, we may categorize the initial SST conditions into three groups: (1) years of large equatorial SST, (2) years of strong cross-equatorial gradient, and (3) neutral years. Note that our intent here is not to argue the physical existence of a dipole-like pattern of SST variability, which has been the subject of intense debate (Houghton and Tourre, 1992; Dommenget and Latif, 2000; Chang et al., 2001). We simply distinguish the years when the cross-equatorial gradient is strong from other years, so that we can examine

the potential importance of the WES feedback in the predictability of tropical Atlantic SST.

The above categorization does not take into consideration the ENSO influence, which has been shown to play an important role in the development of SST anomalies in the TNA. In a recent study, Giannini et al. (2004) have shown that the ENSO influence on the TNA can interfere constructively or destructively with local feedback processes. Constructive interference occurs in those years when the wind-induced latent heat flux remotely forced by an El Niño is in the same phase as the heat flux anomaly induced by the local thermodynamic feedback, and thus the two processes act in concert with one another during the development of the cross-equatorial gradient. Destructive interference occurs in those years when ENSO remote influence and local thermodynamic feedback work against each other. Therefore, the prediction of SST in the tropical Atlantic depends on not only the initial SST condition but also the conditions in the tropical Pacific. To take ENSO into consideration, we first identify ENSO years as those when the December 0/January +1 Niño3.4 index (the average of SST anomalies in (120–170°W, 5°S–5°N)) is larger than 0.75 K. This classification leads to the following warm events: 1963, 1965, 1968, 1969, 1972, 1982, 1986, 1987, 1991, 1994 and 1997, and the following cold events: 1964, 1970, 1973, 1975, 1984, 1988, 1995, 1998, 1999 and 2000 (years refer to the December 0 month). We then combine the ENSO years with the years of large equatorial SST and strong cross-equatorial SST gradient in the tropical Atlantic and categorize the predictions into four groups:

(i) Group 1 (strong gradient with no ENSO): years when the PC time series of EOF 2 exceeds its standard deviation with neutral conditions in the Pacific. These include the negative gradient years (1974 and 1993) and the positive years (1979, 1980, and 1989).
(ii) Group 2 (constructive ENSO interference): years when the SST gradient in the tropical Atlantic is either neutral or of the same sign as expected from ENSO remote influence. These include the constructive El Niño years (1965, 1969, 1987, and 1991) and the constructive La Niña years (1973, 1984, 1988, and 2000).
(iii) Group 3 (destructive ENSO interference): years when the SST gradient in the tropical Atlantic is of the opposite sign to that expected from ENSO remote influence. These include the destructive El Niño years (1963, 1972, 1982, and 1986) and the destructive La Niña years (1995 and 1998).
(iv) Group 4 (large equatorial SST with no ENSO): years when the PC time series of EOF 1 exceeds its standard deviation with neutral conditions in the Pacific. These include warm anomaly years (1962 and 1966) and cold anomaly years (1971, 1976, and 1992).

Note that the above classification may cause ambiguity when the two leading PC time series have comparable amplitudes. In this case, the initial conditions are dominated by both patterns. This ambiguity is more problematic when the PCs have opposite signs. Among all the years used in the composites, only 1962 and 1974 belong to this case. We objectively assigned 1974 to Group 1 and 1962 to Group 4 because the SST in 1974 resembles more closely to EOF2, while in 1962, it resembles more closely to EOF1. The findings presented below, however, are not sensitive to the use of these years: removing them from the groups and using other years instead (in order to compute statistical significance) yields similar results.

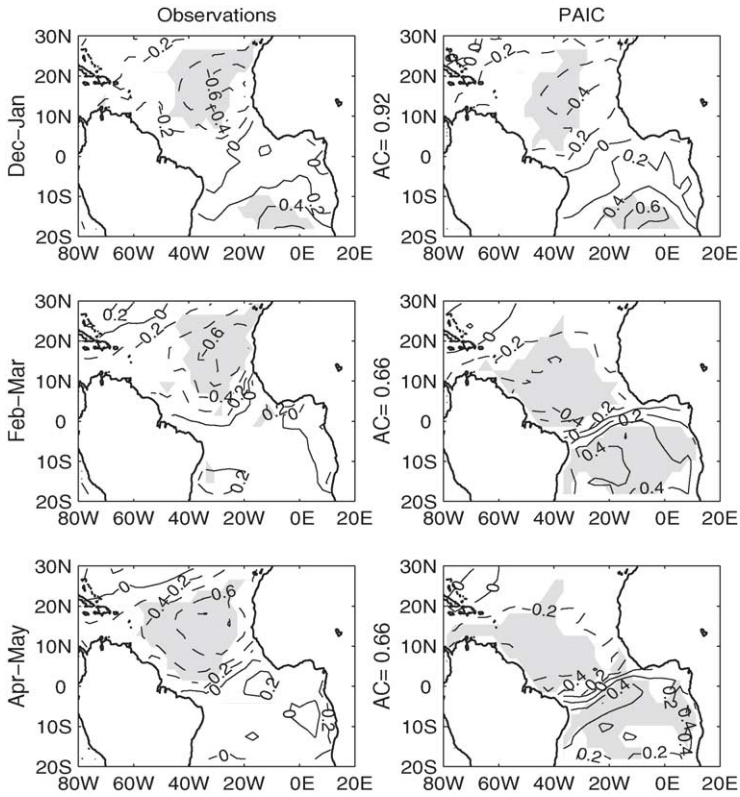

Fig. 4. Composites for strong gradient years with no ENSO (Group 1): observed SST (left panel), PAIC predicted SST (middle panels) and PAIC surface heat flux (right panels). Contour interval for SST is 0.2 K, for heat flux 5 W m^{-2} and shading indicates statistical significance at 95% level. The anomaly correlation (AC) between observed and predicted SST is also displayed.

We expect that PAIC will give skillful SST forecasts for Groups 1 and 2, if the hypothesis that the local feedback plays an important role in the predictable dynamics holds. We further expect that PGIC will give better predictions than PAIC for Group 2, if the hypothesis of the constructive ENSO interference holds. On the other hand, we expect low skills for Groups 3 and 4 because, in these cases, either the local and remote processes that contribute to predictable SST dynamics tend to work against each other or the necessary dynamics for predicting equatorial SST anomaly is absent from the coupled model. We now show that the results presented below support our expectations.

Fig. 4 shows composites of the difference between positive and negative years for Group 1. By construction, the initial conditions depict a large cross-equatorial SST gradient. The subsequent time evolution of the SST pattern predicted by PAIC follows closely the observed pattern, as indicated by the high ($\geq$0.6) pattern correlation, also known as anomaly correlation (AC) (Anderson et al., 1999). In both the observed and predicted fields, the SST evolution shows a strengthening of the cross-equatorial gradient as lead time increases. This

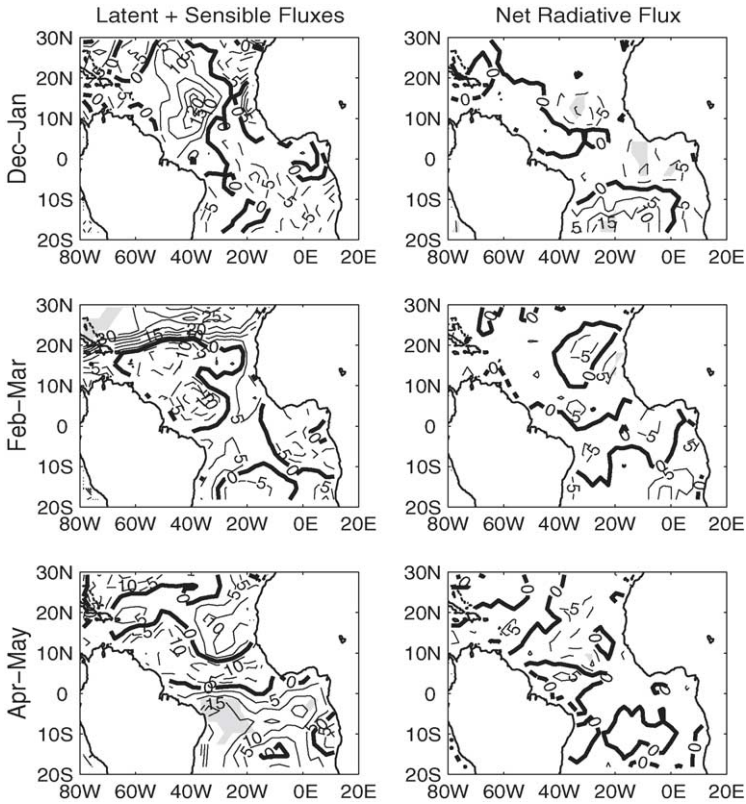

Fig. 5. Composites of observed surface fluxes for strong gradient years with no ENSO (Group 1): latent + sensible heat fluxes (left panel) and net radiative flux (right panels). Contour interval is $5\,W\,m^{-2}$ and shading indicates statistical significance at 95% level.

strengthening in the gradient is accompanied by a westward movement of the maximum SST anomaly in the TNA, which is consistent with the WES feedback mechanism. One noticeable difference between the predicted and observed fields is that the cross-equatorial SST gradient predicted by PAIC is unrealistically strong and tends to be confined too close to the equator compared to the observation. This unrealistic feature can be partially blamed on the absence of ocean processes which can counteract the WES feedback. We shall come back to this issue in Section 3, where a technique is developed to address this problem by including a statistical parameterization of anomalous ocean heat transport in the slab ocean.

Figs. 5 and 6 show the surface heat flux anomalies that accompany the evolution of SST anomalies in the observations and PAIC experiment, respectively. Observed fluxes are taken from the NCEP reanalysis. Although noisy and less statistically significant, observed fluxes show similar features as simulated ones. In both the model and observations, the latent heat flux is larger than the sensible heat flux, and dominates the evolution of SST. The relationship between the latent heat flux and SST is consistent with the WES feedback mechanism. The sign of the flux anomalies from December to March is such that they

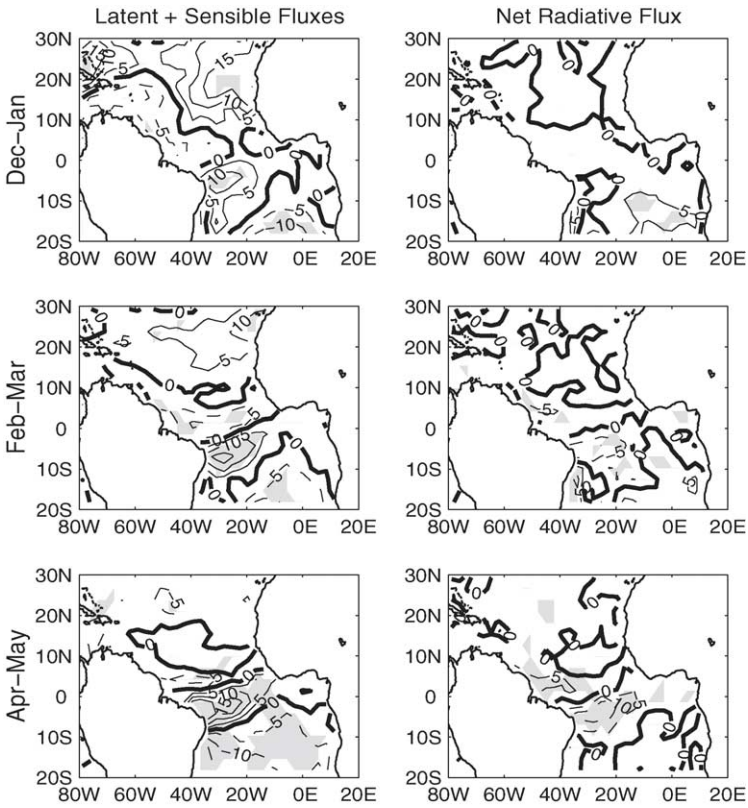

Fig. 6. Composites of PAIC predicted heat fluxes for strong gradient years with no ENSO (Group 1): latent + sensible heat fluxes (left panel) and net radiative flux (right panels). Contour interval is 5 W m^{-2} and shading indicates statistical significance at 95% level.

tend to damp SST anomalies in the northeastern tropical Atlantic, but strengthen them in the western part of the basin (left panels of Fig. 6). This spatial offset between the flux and SST causes an apparent southwestward movement of the TNA SST anomaly towards the deep tropics, where the strongest positive feedback takes place. In the tropical south Atlantic (TSA), the same mechanism moves the center of maximum SST northwestward. The net radiative fluxes are comparatively small. They tend to oppose the positive WES feedback in the deep tropics, mainly due to decreased (increased) solar radiation in regions of enhanced (weakened) rainfall. Until March, the simulated latent heat flux anomalies in the deep tropics are larger than the opposing radiative fluxes, thus strengthening the SST gradient. After March, the predicted net heat flux anomaly changes sign and acts to damp the SST gradient. On the other hand, the observed net heat flux still tends to strengthen the cross-equatorial SST gradient during April–May. Nevertheless, the observed SST gradient has weakened substantially in the next season (not shown), hinting at the importance of ocean dynamics in opposing the surface heat flux.

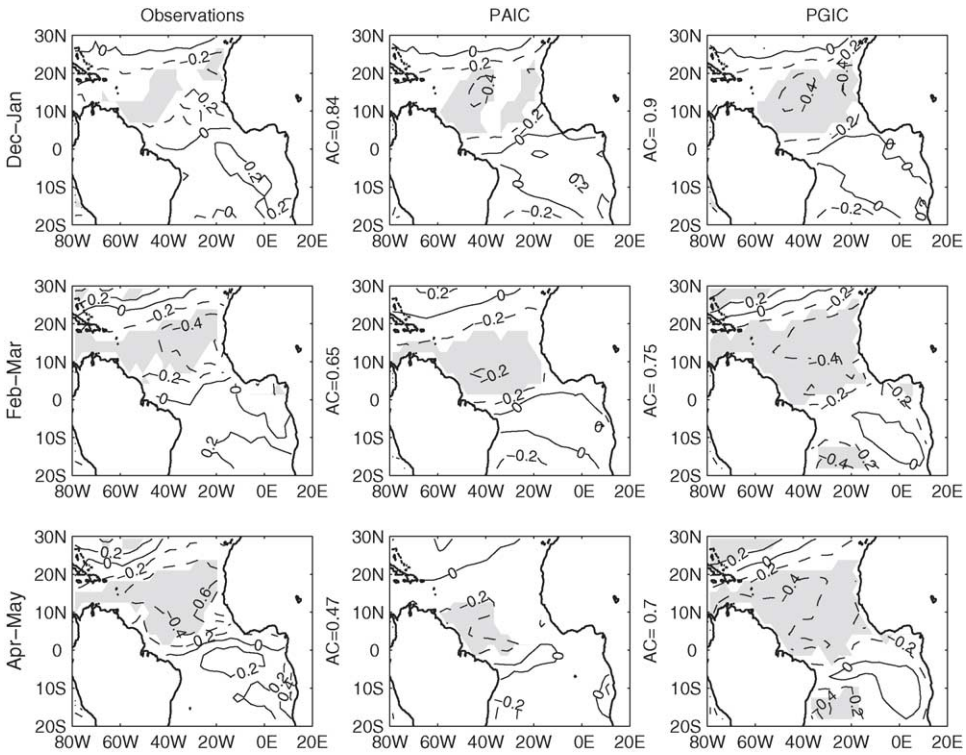

Fig. 7. Composite of SST for years of constructive ENSO interference (Group 2): observed SST (left panels), PAIC predicted SST (middle panels), and PGIC predicted SST (right panels). Contours and shading as in Fig. 4.

There is a region north of 10°N where observed radiative fluxes have the same sign as SST anomalies, suggesting the possibility of a weak positive SST-cloud radiative feedback (Tanimoto and Xie, 2002). This feature, however, is not present in the model. Nevertheless, it occurs in a region that is predicted with a high skill by the model, and thus it does not seem to play a dominant role in SST prediction. In contrast, from the figures, it is evident that the WES feedback plays a leading role in the SST evolution. Therefore, we argue it is this thermodynamic feedback that enhances the skill of the model in predicting the cross-equatorial gradient beyond persistence.

Fig. 7 compares a similar set of observed and predicted SST anomalies for Group 2. For this group, the local feedback and remote ENSO influence positively reinforce one another. Therefore, experiment PGIC, which includes both local and remote dynamics, should give better forecast skills than experiment PAIC, which includes only local dynamics. This is indeed the case. From Fig. 7, it is evident that without the remote ENSO influence, the predicted SST anomalies in the PAIC experiment are too weak compared to the observations, even though the AC retains reasonably high values up to lead times of 6 months. By including ENSO's remote influence, the PGIC experiment improves not only the correlation skill ($AC \geq 0.7$ up to lead times of 6 months) but also the strength of predicted SST anomaly.

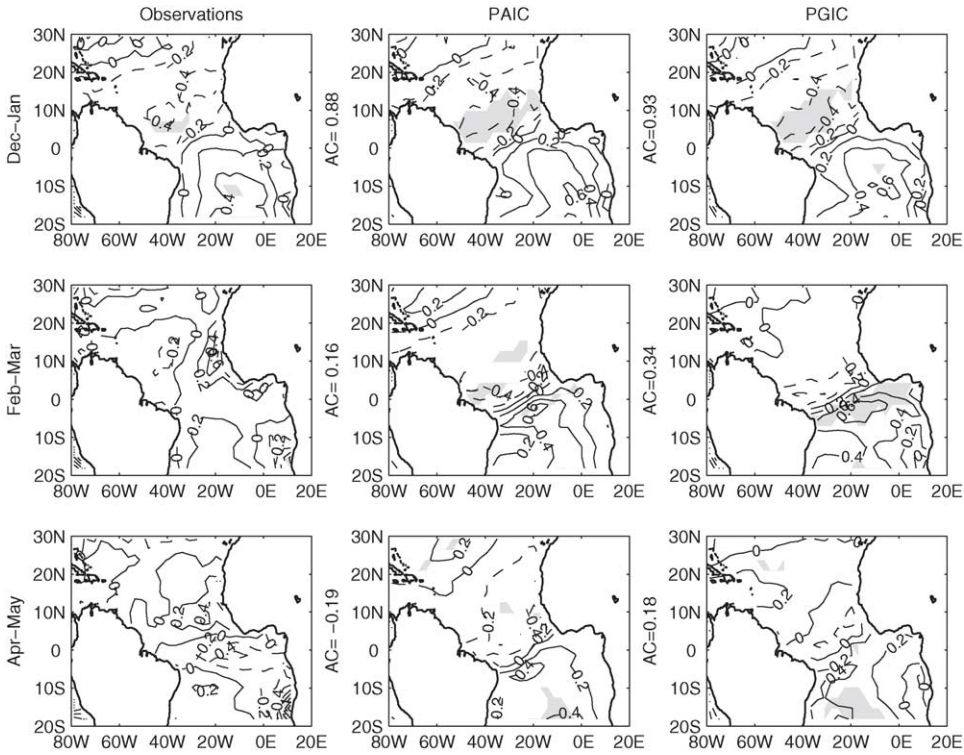

Fig. 8. Same as Fig. 7 years of destructive ENSO interference (Group 3).

Despite the remarkable skill of the model, one major discrepancy is clearly noted: The predicted SSTs have maximum SST anomalies in the western TNA, whereas the large SST anomalies in the observation tend to occur in the eastern TNA off the coast of Africa where the upwelling is intense. This points to the potential importance of upwelling dynamics that are missing from the slab ocean model.

Fig. 8 shows the composite of Group 3, where ENSO's remote influence tends to work against the local feedback. In this case, the fate of the SST anomalies after December depends on the relative importance of the local feedback and ENSO remote influence. In the PAIC experiment where ENSO remote influence is absent, the model predicts that the initial SST gradient persist through spring due to the WES feedback, whereas in reality, the ENSO's remote influence overpowers the local feedback, reversing the spring SST gradient. Therefore, the PAIC experiment has essentially no skill 2 months into the prediction. In the PGIC experiment, where ENSO remote influence is present, the model has the correct tendency to reverse the initial SST gradient. But, apparently, the remote effect of ENSO in the model is not strong enough to overcome the initial SST gradient. The skill of the prediction, though improved over PAIC, is still quite low compared to previous cases. This result illustrates the potential difficulty of predicting Atlantic SST when ENSO destructively interferes with the local dynamics. The successful prediction in this case requires that the

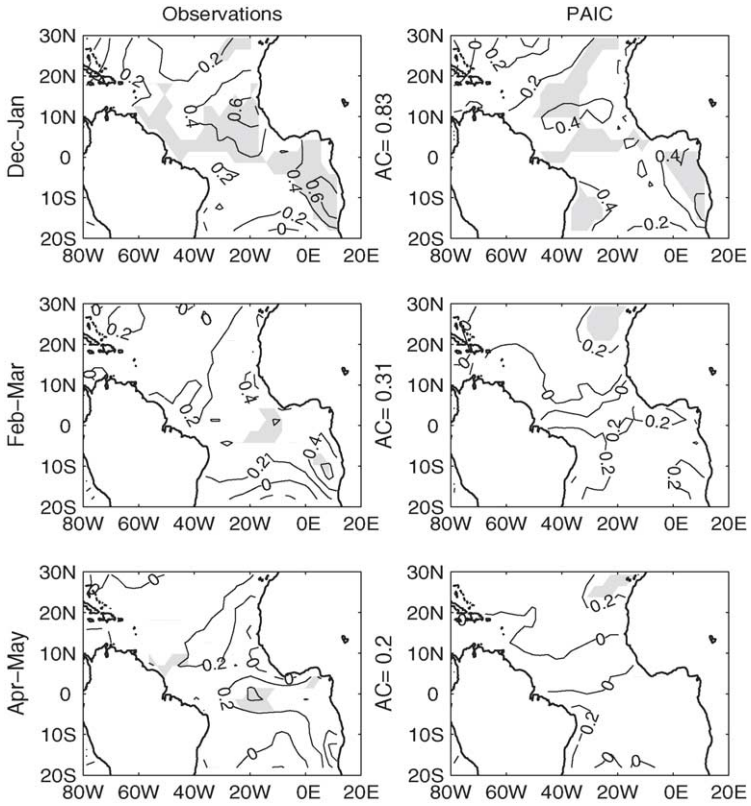

Fig. 9. Composite of SST for years with large equatorial SST (Group 4): observations (left panels) and PAIC (right panels). Contours and shading as in Fig. 4.

model not only includes both the local and remote dynamics but also has the capability to predict the relative strength of each process.

Finally, we consider the composite for Group 4, where the initial SST has a large anomaly in the equatorial and cold tongue regions of the Atlantic. Since the coupled model contains no ocean dynamics, we expect that the predictions will fail miserably. This is indeed the case. The SST composite for this case is shown in Fig. 9. The initial condition in December presents positive SST anomalies over the entire basin with large weight in the cold tongue region and weak cross-equatorial SST gradient. There is no evidence of thermodynamic feedback in the PAIC experiment to support the SST evolution and the initial SST anomaly decays rapidly. After 2 months, there are practically no SST anomalies in the model and the AC values are low. This suggests that in the absence of any initial cross-equatorial gradient, the coupled model cannot sustain any growth of SST anomalies. The SST evolution in this case appears to obey the zero-dimensional Hasselmann model in which the SST variability is described as the integrated effect of atmospheric noise (Hasselmann, 1976). Interestingly, the observed SST also tends to decay with time. The equatorial anomalies tend to persist

longer than in the off-equatorial region, hinting of the importance of ocean dynamics in the variability of SST for these years.

In summary, the results presented in this section support the hypothesis that the local positive air–sea feedback and the remote ENSO influence play a crucial role in predicting the cross-equatorial SST gradient anomaly in the tropical Atlantic during boreal spring. The local feedback works most effectively when there is a cross-equatorial SST gradient during boreal winter. It acts to enhance the initial gradient in the deep tropics. ENSO can interfere with the local feedback constructively or destructively. The constructive interference enhances the forecast skill of the model, whereas the destructive interference decreases the model's ability to forecast. The results presented in this section further hint at the potential importance of ocean dynamics in the prediction of tropical Atlantic SST, which is entirely missing in the standard CCM3-ML model. For example, during the destructive ENSO years (Group 3) and the years when the equatorial mode dominates the initial SST condition (Group 4), there is a well-defined SST anomaly developed in the equatorial south Atlantic in the late spring that is not captured by the standard model. There is evidence that the SST gradient is exaggerated in the PAIC experiment, which may also be related to the lack of ocean physics. These observations motivate us to further investigate on the role of ocean dynamics in predicting tropical Atlantic SST from winter into spring.

3. Role of ocean dynamics

In order to investigate the role of ocean dynamics, we introduce a new term to the slab ocean model SST equation that parameterizes the ocean heat transport due to anomalous ocean dynamics. We assume that the missing ocean dynamics are linear, and can be parameterized in terms of the SST anomaly, as $\mathbf{B}T$, where $\mathbf{B}$ is a linear operator representing the missing ocean dynamics, and T the model temperature anomalies. $\mathbf{B}$ can be determined using a Linear Inverse Modeling procedure (Penland and Sardesmukh, 1995) that is presented in the Appendix. The correction procedure was applied to the equatorial and tropical south atlantic (ETSA) in the region defined by (50°W–20°E, 20°S–5°N). This is the area where the standard CCM3-ML model consistently shows low skill. The existing literature (Carton and Huang, 1994) also points to this region as being sensitive to changes in ocean conditions. Upon introduction of $\mathbf{B}T$ into the slab ocean, the linearized SST equation reads

$$\frac{\partial T}{\partial t} = \mathbf{A}T + \mathbf{B}T + Q_N \tag{1}$$

where T denotes the SST anomaly, matrix $\mathbf{A}$ represents the coupled thermodynamic ocean–atmosphere feedback in the standard model, and Q_N are the surface heat fluxes induced by internal atmospheric variability and not coupled to SST anomalies. Setting $\mathbf{B}T$ to zero in the above equation gives back the linear dynamics of the slab ocean used in the PAIC and PGIC experiments. In practice, $\mathbf{B}T$ represents not only the missing ocean dynamics but also systematic errors in the atmospheric fluxes of the model. Moreover, the correction may also compensate for effects such as using a time-mean mixed layer depth. (The mean value of the mixed layer depth in ETSA is 33 m, with a seasonal variation of about 40% of the mean value.) We assume that the latter are smaller than the former, so

that **B** represents, to a large degree, the missing ocean dynamics. Results presented below suggest that the correction can indeed be interpreted in this way.

To test the importance of ocean dynamics, we repeat ensembles of prediction experiments similar to PAIC and PGIC, but with the inclusion of **B***T*. These new experiments are referred to as CPAIC and CPGIC. The new experiments were carried out only for the period 1981–2000 because of the concern of data quality in the Southern Hemisphere prior to 1981 when satellite-derived SST are not available.

Before proceeding to discuss the results of the new experiments, it is worth mentioning that **B** is generally non-diagonal. This means the correction introduced into the slab ocean is non-local. That is, changes of SST in one location due to **B***T* depend on SST anomalies in other locations. This property is essential to represent dynamical ocean processes, which can affect remote areas through advection or wave propagation.

3.1. Skill of the corrected models

Fig. 10 compares the SST correlation maps of the standard model prediction experiments (PAIC, PGIC) and the corrected model experiments (CPAIC, CPGIC) during MAM. The correlations are calculated for the period 1981–2000. While the skill in the TNA region is, as expected, largely unaffected by the correction, there is a noted difference in the model

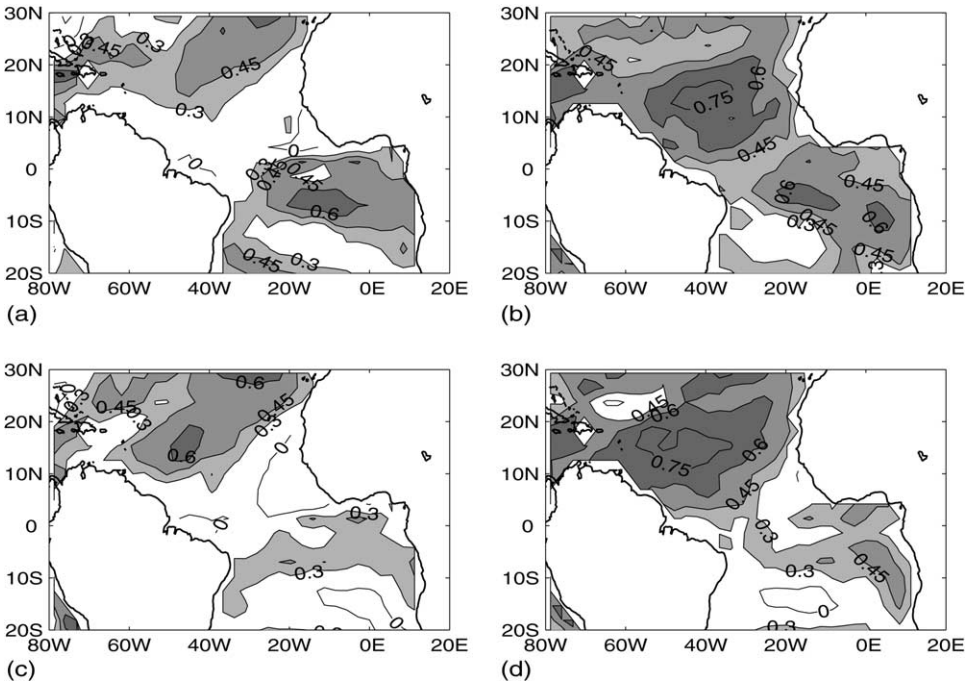

Fig. 10. Correlation skill of SST for the four prediction experiments in MAM during 1981–2000. (a) CPAIC, (b) CPGIC, (c) PAIC, and (d) PGIC.

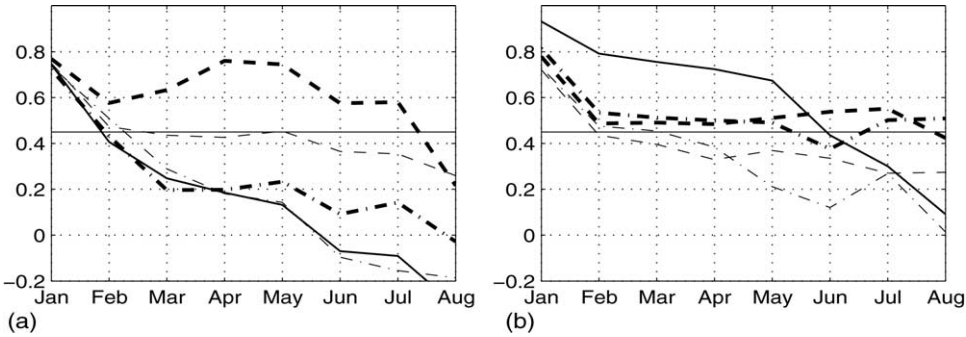

Fig. 11. Correlation between predicted and observed (a) gradient index and (b) ATL3 index for each prediction experiment: PAIC (dashed–dotted line), PGIC (dashed line), CPAIC (bold dashed–dotted line), and CPGIC (bold dashed line). Persistence of the index is shown as a solid line. The horizontal line denotes the 95% significance level.

forecast skill in the equatorial and tropical south Atlantic (ETSA), particularly in the cold tongue region. The predictions with the corrected model are clearly superior to those of the standard model. Both the CPGIC and CPAIC show larger areas in the south tropical Atlantic where correlation skill is higher than 0.45, which is significant at the 95% level. The higher skill of the corrected predictions in the ETSA actually extends into the following season (not shown).

To further compare the corrected and standard model skill, we constructed an index to characterize the meridional mode. This so-called gradient index is defined as the SST difference between the regions defined by (50°–20°W, 4°–14°N) and (35°–5°W, 4°–14°S). Fig. 11a shows the correlation of the gradient index constructed for each prediction experiment with the observed index. By this measure, it is evident that (1) higher predictive skill is achieved when the model is initialized with global SST and (2) the corrected model has better skill than the standard model. The latter is particularly evident when comparing CPGIC to PGIC: PGIC gives a correlation skill of about $r = 0.45$ from February to May that is just at the 95% significance level. CPGIC, on the other hand, possesses correlation skill well above the 95% significance level with a peak value of $r \simeq 0.75$ during April–May. This value is significant at the 99% level. The improved correlation skill during MAM coincides with the peak season of the gradient mode, suggesting that ocean dynamics is an important player in the evolution of the meridional mode and can work in concert with the local thermodynamic feedback and ENSO remote influence to enhance the predictability of the cross-equatorial SST gradient anomaly.

Does the included ocean dynamics also improve the predictability of the equatorial mode? To address this issue, we constructed the ATL3 index, which is defined as the average of the SST anomaly in the region (20°W–0°E, 3°S–3°N) (Zebiak, 1993). The correlation of the predicted ATL3 index with observations is shown in Fig. 11b. Although the corrected model tends to improve the skill over the standard model in this region, none of the predictions beats the persistence forecast up to lead times of 6 months. Only at the longer lead times is the skill of the corrected model superior to persistence. It is also interesting to note that unlike the gradient index, there is no significant difference between

the experiments initialized with the global SST and the Atlantic SST. The absence of this difference suggests that SST variability in the ATL3 region is not strongly affected by ENSO remote influences. The fact that the corrected model's skill is lower than persistence indicates that this simple correction is not sufficient to capture the complex dynamics of the equatorial mode. That said, it should also be noted that the equatorial mode primarily manifests itself during the boreal summer. The prediction experiments presented here begin in boreal winter. The failure of the model in this season does not necessarily mean the failure of the model in other seasons. Nevertheless, the mechanisms that give rise to long persistence of the SST anomaly in the ATL3 region are worth noting and deserve further study.

3.2. Physical interpretation

As mentioned earlier, the standard model performed poorly for the case of destructive ENSO interference (Group 3). The failure of the model was argued to be caused by the exaggerated thermodynamic feedback due to lack of ocean dynamics. Therefore, it is instructive to compare the SST evolutions predicted by the corrected and standard models for Group 3 to see whether and how the parameterized ocean dynamics can improve the prediction. We consider the subset of years of Group 3 that lies within the period 1981–2000. It consists of two El Niño years (1982 and 1996) and two La Niña years (1995 and 1998).

Fig. 12 shows the time evolution of the SST composite for the observations, CPGIC and PGIC from December to May. Surface wind vectors are superimposed on the SST anomalies to illustrate the coupling between the atmosphere and ocean. These winds are taken at 925 mb from both the NCEP reanalysis data and the CCM3. The evolution of SST anomalies in the observations and the standard model (PGIC) is very similar to Fig. 8: while in the observations the remote ENSO influence changes the sign of the cross-equatorial SST gradient from December to May, in the standard model the ENSO influence cannot affect the deep tropics. As a result, in April–May, PGIC shows the wrong cross-equatorial SST gradient and the predicted surface winds flow in the wrong direction. This is, as pointed out before, a consequence of an exaggerated local thermodynamic feedback in PGIC. In reality, this feedback and the growth of the meridional mode are suppressed by both the remote ENSO influence and the dynamic feedback in the eastern equatorial cold tongue region. The corrected model attempts to capture the dynamic feedback in the cold tongue region, while the standard model misses this effect completely. Thus, while the standard model (PGIC) falsely predicted a strong gradient anomaly in the western tropical Atlantic, the corrected model (CPGIC) correctly predicted the negative SST anomaly in the cold tongue region during April–May.

It is further interesting to note that although the corrected model gives a much more realistic prediction in April–May than the standard model, it misses the prediction in February–March when the SST gradient reverses its direction in reality. This indicates that the corrected model still overestimates the strength of the thermodynamic feedback in the equatorial region. Therefore, the results shown here indicate that the ocean dynamics can act to oppose the thermodynamic feedback. The weakening of the thermodynamic feedback, in turn, allows the remote ENSO influence to affect the deep tropics. These results show that predicting SST anomaly in the equatorial and south tropical Atlantic requires

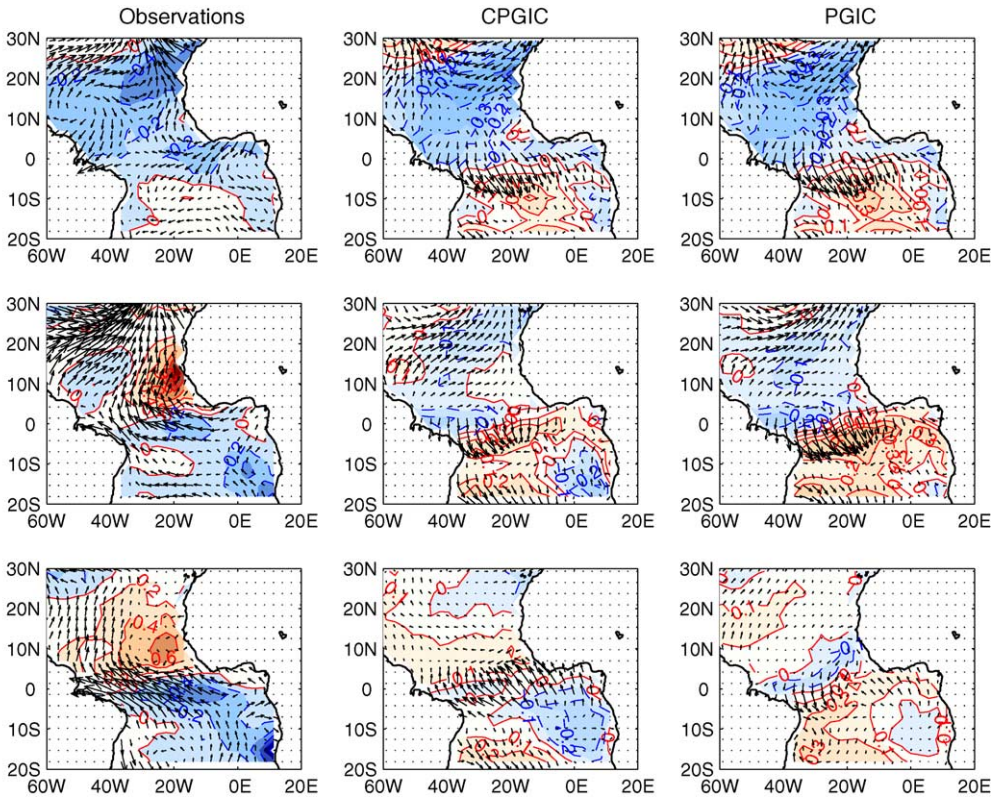

Fig. 12. Composite of SST and surface winds for observations (left panels), CPGIC (middle panels) and PGIC (right panels) during the destructive interference El Niño years (1982 and 1986) and La Niña years (1995 and 1998). Note that in the left panels the SST contours are 0.2 K, while in the other panels, the contours are 0.1 K.

a model that is capable of simulating realistically both the thermodynamic and dynamic feedbacks, as well as the remote influence of ENSO.

A similar analysis could be repeated for the years of Group 4, that is, for those years having initial SST anomaly with a large amplitude in the equatorial region. However, during the period 1981–2000, only 1 year, 1992, belongs to this group (see Section 2.2), and thus the composite analysis can not be performed.

The results so far indicate that the correction term is effective in improving the prediction of the model. The next logical question to ask is, what ocean processes are parameterized in matrix **B**? This question can be at least partially answered by determining the ocean dynamics responsible for the observed equatorial SST anomaly in the composite shown in Fig. 12. This requires a careful analysis of the mixed layer heat budget, which is beyond the scope of this study. We defer a comprehensive heat budget analysis to a later study. Here, we present a simple and less complete analysis that suggests that the Ekman pumping term seems to play an important role in the evolution of equatorial SSTs, and thus it may be one of the key ocean dynamics parameterized in **B**.

Consider a linearized temperature equation:

$$\frac{\partial T'}{\partial t} = -\bar{u}\frac{\partial T'}{\partial x} - \bar{v}\frac{\partial T'}{\partial y} - \bar{w}\frac{\partial T'}{\partial z} - u'\frac{\partial \bar{T}}{\partial x} - v'\frac{\partial \bar{T}}{\partial y} - w'\frac{\partial \bar{T}}{\partial z} + Q'. \tag{2}$$

The advective terms in Eq. (2) involve the velocity $\boldsymbol{u}$ of the upper ocean, which can be decomposed into an Ekman and a geostrophic part. Here, we assume that the Ekman part dominates over the geostrophic part, and thus only the former is considered. Following Zebiak and Cane (1987), we then compute the horizontal Ekman transport ($U_{\mathrm{E}}^{\mathrm{H}} = \int_{-H}^{0} u_{\mathrm{E}}^{\mathrm{H}} \mathrm{d}z$) as follows,

$$U_{\mathrm{E}}^{\mathrm{H}} = (U_{\mathrm{E}}, V_{\mathrm{E}}) = \frac{1}{\rho(f^2+\gamma^2)}(f\tau_y + \gamma\tau_x,\ -f\tau_x + \gamma\tau_y), \tag{3}$$

where H is the depth of the mixed layer, ρ is the density of ocean water, $\tau = (\tau_x, \tau_y)$ the wind stress, and f the Coriolis parameter. The parameter γ is the damping time scale associated with the frictional term included in the balance. We used a value of $\gamma = 0.5$ per day as in

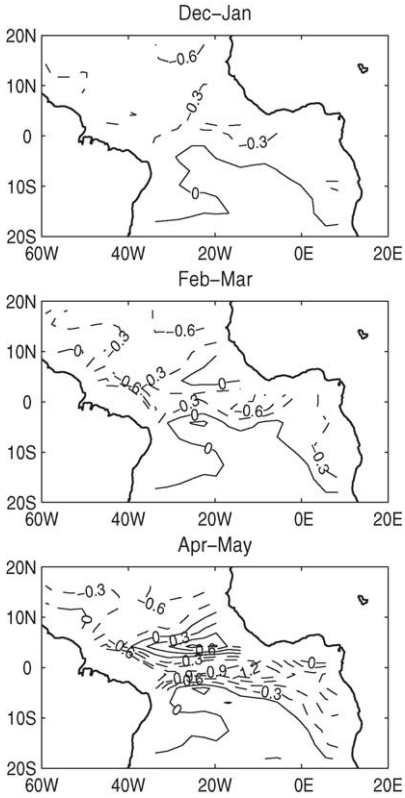

Fig. 13. Composite of the contribution of Ekman pumping to SST evolution. The composite is constructed using the same years of Fig. 12.

Zebiak and Cane (1987) and Sterl and Hazeleger (2003). The Ekman pumping velocity is calculated as the horizontal divergence of the Ekman transport, i.e., $w_{\mathrm{E}} = \nabla \cdot U_{\mathrm{E}}^{\mathrm{H}}$. The climatological vertical temperature gradient and the mixed layer depth are calculated using the annual mean conditions of an ocean data assimilation (ODA) product (Harrinson, 2002). Since all the Ekman terms are linearly related to the surface wind stresses, we can calculate each of the tendency terms directly from the wind stresses given by the NCEP reanalysis, except for the term $\overline{w}\frac{\partial T'}{\partial z}$, which is not calculated here. We do not imply the latter term is not important, but its role will be addressed in future work. The results show that the largest term is the anomalous Ekman pumping. A separation of Ekman pumping into contributions from the zonal and meridional wind stresses indicates that the zonal wind stress anomaly has the dominant effect. To illustrate the importance of Ekman pumping, Fig. 13 shows a composite of the SST evolution solely given by the Ekman pumping term, $w'_{\mathrm{E}}\frac{\partial \overline{T}}{\partial z}$. Clearly, the evolution of the equatorial SST follows that of the observed SST. In the central Atlantic, the shape and evolution of the SST anomaly bears a reasonable resemblance to the observations. Note, however, the magnitude of the SST anomaly given by the Ekman pumping term is larger than the observed one, suggesting that other terms in the SST tendency equation tend to oppose it. It is also worth noting that the Ekman pumping does not play an important role in the off-equatorial regions where surface heat flux tends to dominate the SST variability. Overall, this analysis suggests that the linear correction $\mathbf{B}T$ includes a parameterization of the temperature changes due to the anomalous Ekman pumping term.

4. Summary

In this study, we investigated the dynamical processes that contribute to the predictability of SST in the tropical Atlantic from boreal winter to spring. With an atmospheric general circulation model coupled to a slab ocean, we first tested the hypothesis that both the local feedback and the remote ENSO influence contribute to the predictability of SSTs. By a careful examination of the dependence of the model forecast skill on the initial SST conditions in both the tropical Atlantic and tropical Pacific, we showed that (1) the WES feedback mechanism is a major contributing factor in enhancing the spring SST predictability beyond persistence in the absence of the remote ENSO influence and (2) the remote ENSO influence may act constructively or destructively with this local feedback. In the case of a constructive interference, both processes tend to work together to create a strong and persistent cross-equatorial SST gradient anomaly, thus giving rise to high forecast skill of the coupled model. On the other hand, when ENSO interacts destructively with the local feedbacks, the skill of the model is generally poor, because it requires that the model not only simply includes both the local and remote dynamics but also have the ability to capture the relative strength of each process.

Taking advantage of the simplicity of the ocean physics in the coupled model, we then investigated the role of ocean dynamics in the predictability of SST anomalies associated with the meridional mode. The low skill of the model in the ETSA region leads us to hypothesize that the absence of ocean dynamics in the model is a major factor responsible for

the low skill. To test this hypothesis, we developed a methodology to introduce a statistical correction to the slab ocean that parameterizes the missing anomalous heat transport due to ocean dynamics. We showed that the predictions with the corrected model outperform the standard model in the ETSA region particularly at long lead times. This points to the importance of ocean dynamics in the prediction of tropical Atlantic SSTs. A simple diagnostic analysis of the SST evolution suggests that the anomalous Ekman pumping is particularly important to predictable dynamics for the SST in the equatorial region. The role of the ocean process during MAM is to weaken the positive thermodynamic air–sea feedback between SST and heat flux in the equatorial region. This finding is consistent with the observational study of Chiang et al. (2002), who proposed that while the role of the positive feedback is to sustain the SST gradient during boreal spring, the ocean heat transport in the equatorial region works against it preventing the gradient to persist into the next season.

We would like to note that even with the correction term included, the skill of the model south of 10°S is relatively low. We speculate that one of the reasons for the low skill is a poor representation of the stratus cloud deck in the southern subtropics and the associated SST-cloud radiative feedback in the model (Tanimoto and Xie, 2002).

We end this study by addressing a more practical question: how useful is the reduced-physics coupled model in predicting boreal spring rainfall anomaly in the region? It is well known that MAM marks the rainy season over the north Northeastern region of Brazil, which extends over (35–45°W, 2–10°S) (Hastenrath, 1985). Given the skill of the model in predicting SST anomaly in the season, it is natural to ask how much of the SST forecast skill can be translated to seasonal precipitation forecasts in the tropical Atlantic. To address this issue, we computed the correlation between observed and predicted rainfall for CPGIC experiment during MAM over the period 1982–2000. Fig. 14 shows a comparison of the potential skill of CCM3 in predicting rainfall anomaly to the actual skill of the corrected CCM3-ML during MAM for the entire tropical Atlantic region. The correlation skill of PGIC is lower and is not shown. Potential predictability in Fig. 14b is derived from an ensemble of CCM3 integrations forced by the observed SST from 1979 to 1994 (GOGA runs),

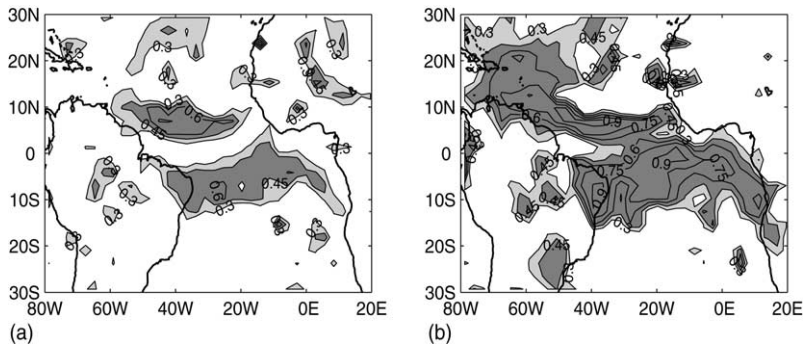

Fig. 14. Correlation between predicted and observed rainfall for (a) CPGIC and (b) GOGA during MAM. The contour interval is 0.15. Light shading indicates values above $r = 0.3$ and dark shading indicates values above $r = 0.45$.

and defines the upper limit of the model skill because it assumes that the SST is predicted perfectly. Clearly, the simple coupled model has considerable skill. A rough estimate indicates that the model predictions made two seasons in advance can capture approximately 30–40% of the observed rainfall variance. In comparison, the potential predictability captures about 60–70%. Given the current state of seasonal climate forecast in the tropical Atlantic sector, the skill of this simple system is highly encouraging.

Appendix A Methodology to correct the slab ocean

The evolution of SST anomalies in the slab ocean is determined by $\frac{\partial T}{\partial x} = Q$ where T is the sea-surface temperature anomaly, and Q is the net surface heat flux anomaly into the ocean divided by the heat capacity of the mixed layer. The total heat flux is separated into two contributions: one that is related to the surface temperature ($Q_S(T)$), and a second part that is due to internal atmospheric variability (Q_N). We further consider $Q_S(T) = \mathbf{A}T$, where $\mathbf{A}$ is generally a non-diagonal matrix representing ocean–atmosphere thermodynamic feedbacks.

Assume that the evolution of observed SST can also be described by an analogous equation with $\hat{Q}_S(\hat{T}) = \hat{\mathbf{A}}\hat{T}$ (the "hat" denotes observed quantities). Matrix $\hat{\mathbf{A}}$ is different from $\mathbf{A}$ because the former includes a contribution from ocean dynamics. The goal is to derive a matrix $\mathbf{B}$, such that $\mathbf{A} + \mathbf{B}$ approximates $\hat{\mathbf{A}}$ as close as possible. After the operator $\mathbf{B}$ is determined, we can incorporate it into the equation of the slab ocean. The new term $\mathbf{B}T$ will represent an anomalous ocean heat transport.

To find $\mathbf{B}$, we construct an equation for the prediction error $\epsilon = \hat{T} - T$ taking the difference between the equations for observed and predicted SST. This leads to

$$\frac{\partial \epsilon}{\partial t} = \hat{\mathbf{A}}\epsilon + \mathbf{B}T + \zeta, \tag{A.1}$$

where ζ is white noise. Integrating this equation for a short lead time τ, and multiplying by the initial condition $T(0)$, allows to calculate $\mathbf{B}$ as the coefficient matrix of a multivariate linear regression

$$\mathbf{B} = \frac{1}{\tau}\langle \epsilon(\tau)T(0)^t \rangle \langle T(0)T(0)^t \rangle^{-1}, \tag{A.2}$$

where the brackets denote a time average.

The calculation of $\mathbf{B}$ involves finding the inverse of the December SST covariance matrix, which is singular. To solve this problem, we worked in the EOF space of December SST. After performing several sensitivity tests by varying the EOF truncation and the lead time τ, $\mathbf{B}$ was calculated truncating at four EOFs (82% of the total variance) and using $\tau = 1$ month.

References

Anderson, J., van den Dool, H., Barnston, A., Chen, W., Stern, W., Ploshay, J., 1999. Present-day capabilities of numerical and statistical models for atmospheric extratropical seasonal simulation and prediction. Bull. Am. Meteorol. Soc. 80, 1349–1362.

Carton, J.A., Huang, B.H., 1994. Warm events in the tropical Atlantic. J. Phys. Oceanogr. 24, 888–903.

Chang, P., Ji, L., Saravanan, R., 2001. A hybrid coupled model study of Tropical Atlantic Variability. J. Clim. 14, 361–390.

Chang, P., Saravanan, R., Ji, L., Hegerl, G., 2000. The effect of local sea surface temperature on atmospheric circulation over the tropical sector. J. Clim. 13, 2195–2216.

Chiang, J.C.H., Kushnir, Y., Giannini, A., 2002. Deconstructing Atlantic ITCZ variability: influence of the local cross-equatorial SST gradient, and remote forcing from the eastern equatorial Pacific. J. Geophys. Res. 107, 1–19.

Czaja, A., van der Vaart, P., Marshall, J., 2002. A diagnostic study of the role of remote forcing in tropical Atlantic variability. J. Clim. 15, 3280–3290.

Davey, M.K., et al., 2002. STOIC: a study of coupled model climatology and variability in tropical ocean regions. Clim. Dyn. 18, 403–420.

Dommenget, D., Latif, M., 2000. Interannual to decadal variability in the tropical Atlantic. J. Clim. 13, 777–792.

Enfield, D.B., Mayer, D.A., 1997. Tropical Atlantic sea surface temperature variability and its relation to El Niño-Southern Oscillation. J. Geophys. Res. 102, 929–945.

Folland, C., Palmer, T., Parker, D., 1986. Sahel rainfall and worldwide surface temperatures: 1901–1985. Nature 320, 602–606.

Giannini, A., Saravanan, R., Chang, P., 2004. The preconditioning role of Tropical Atlantic Variability in the development of the ENSO teleconnection: implications for the prediction of Nordeste rainfall. Clim. Dyn. 22, 839–855.

Goddard, L., Mason, S.J., Zebiak, S.E., Ropelewsky, C.F., Basher, R., Cane, M.A., 2001. Current approaches to seasonal-to-interannual climate predictions. Int. J. Climatol. 21, 1111–1152.

Harrinson, M. J., 2002. Ocean data assimilation and experiments. Geophysical Fluid Dynamics Laboratory: Climate Dynamics & Prediction, http://www.gfdl.noaa.gov/∼kd/ClimateDynamics/climate.html.

Hasselmann, K., 1976. Stochastic climate models: I. Theory. Tellus 28, 473–485.

Hastenrath, S., 1985. Climate and Circulation of the Tropics. D. Reidel, Boston, 455 pp.

Hastenrath, S., Heller, L., 1977. Dynamics of climate hazards in northeast Brazil. Quart. J. Roy. Meteor. Soc. 103, 77–92.

Houghton, R.W., Tourre, Y., 1992. Characteristics of low frequency sea surface fluctuations in the tropical Atlantic. J. Clim. 5, 765–771.

Kalnay, E., et al., 1996. The NCEP/NCAR 40-Year Reanalysis Project. Bull. Am. Meteorol. Soc. 77, 437–471.

Kiehl, J.T., Hack, J., Bonan, G.B., Boville, B.P., Williamson, D.L., Rasch, P.J., 1998. The National Center for Atmospheric Research Community Climate Model: CCM3. J. Clim. 11, 1131–1149.

Klein, S.A., Soden, B.J., Lau, N.-C., 1999. Remote sea surface temperature variations during ENSO: evidence for a tropical atmospheric bridge. J. Clim. 12, 917–932.

Levitus, S., 1994. World ocean atlas CD-ROM data sets. National Oceanographic Data Center Ocean Climate Laboratory.

Murtugudde, R., Ballabrera, J., Beauchamp, J., Busalacchi, A., 2002. Relationship between zonal and meridional modes in the tropical Atlantic. Geophys. Res. Lett. 22, 4463–4466.

Penland, C., Matrosova, L., 1998. Prediction of tropical Atlantic sea surface temperatures using Linear Inverse Modeling. J. Clim. 11, 483–496.

Penland, C., Sardesmukh, P., 1995. The optimal growth of tropical sea surface temperature anomalies. J. Clim. 8, 1999–2024.

Ruiz-Barradas, A., Carton, J.A., Nigam, S., 2000. Structure of interannual-to-decadal climate variability in the tropical Atlantic sector. J. Clim. 13, 3285–3297.

Saravanan, R., Chang, P., 2000. Interaction between tropical Atlantic variability and El Niño-Southern Oscillation. J. Clim. 13, 2177–2194.

Seager, R., Kushnir, Y., Chang, P., Naik, N., Miller, J., Hazeleger, W., 2001. Looking for the role of the ocean in tropical Atlantic decadal climate variability. J. Clim. 14, 638–655.

Servain, J., Wainer, I., McCreary, J., Dessier, A., 2001. Relationship between the equatorial and meridional modes of climatic variability in the tropical Atlantic. Geophys. Res. Lett. 26, 485–488.

Smith, T.M., Reynolds, R.W., Livezey, R.E., Stokes, D.C., 1996. Reconstruction of historical sea surface temperatures using empirical orthogonal functions. J. Clim. 9, 1403–1420.

Sterl, A., Hazeleger, W., 2003. Coupled variability and air–sea interaction in the South Atlantic Ocean. Clim. Dyn. 21, 559–571.

Tanimoto, Y., Xie, S.-P., 2002. Inter-hemispheric decadal variations in SST, surface wind, heat flux and cloud cover over the Atlantic Ocean. J. Meteor. Soc. Jpn. 80, 1199–1219.

Zebiak, S.E., 1993. Air–sea interaction in the equatorial Atlantic region. J. Clim. 6, 1567–1586.

Zebiak, S.E., Cane, M., 1987. A model El Niño-Southern Oscillation. Monthly Weather Rev. 115, 2262–2278.